Title:

Determining major factors controlling phosphorus removal by promising adsorbents used for lake restoration: a linear mixed model approach

Authors: A. Funes[a,b*], F. J. Martínez[a], I. Álvarez-Manzaneda[a,b], J.M. Conde-Porcuna[a,b], J. de Vicente [c], F. Guerrero[d,e] and I. de Vicente[a,b]

Affiliations:

(a) Departamento de Ecología, Facultad de Ciencias, Universidad de Granada, 18071, Granada (Spain)

(b) Instituto del Agua, Universidad de Granada, 18071, Granada (Spain)

(c) Departamento de Física Aplicada, Facultad de Ciencias, Universidad de Granada, 18071, Granada (Spain)

(d) Departamento de Biología Animal, Biología Vegetal y Ecología, Universidad de Jaén, 23071 Jaén (Spain)

(e) Centro de Estudios Avanzados en Ciencias de la Tierra, Universidad de Jaén, 23071 Jaén (Spain)

Full address for correspondence:

[*]Corresponding author:

Departamento de Ecología, Facultad de Ciencias, Universidad de Granada, 18071, Granada (Spain)

Phone: (+34) 958 248323; Fax: (+34) 958 243093; email: afunes@ugr.es

Abstract

Phosphorus (P) removal from lake/drainage waters by novel adsorbents may be affected by competitive substances naturally present in the aqueous media. Up to date, the effect of interfering substances has been studied basically on simple matrices (single-factor effects) or by applying unsuitable statistical approaches when using natural lake water. In this study, we determined major factors controlling P removal efficiency in 20 aquatic ecosystems in the southeast Spain by using linear mixed models. Two non-magnetic -CFH-12® and Phoslock®- and two magnetic materials -hydrous lanthanum oxide loaded silica-coated magnetite (Fe-Si-La) and commercial zero-valent iron particles (FeHQ)- were tested to remove P at two adsorbent dosages. Results showed that the type of adsorbent, the adsorbent dosage and color of water (indicative of humic substances) are major factors controlling P removal efficiency. Differences in physico-chemical properties (i.e. surface charge or specific surface), composition and structure explain differences in maximum P adsorption capacity and performance of the adsorbents when competitive ions are present. The highest P removal efficiency, independently on whether the adsorbent dosage was low or high, were 85-100% for Phoslock and CFH-12®, 70-100% for Fe-Si-La and 0-15% for FeHQ. The low dosage of FeHQ, compared to previous studies, explained its low P removal efficiency. Although non-magnetic materials were the most efficient, magnetic adsorbents (especially Fe-Si-La) could be proposed for P removal as they can be recovered along with P and be reused, potentially making them more profitable in a long-term period.

Keywords: phosphorus, magnetic particles, Phoslock®, CFH-12®, linear mixed model, lake restoration.

Introduction

Sewage, industrial discharge and agricultural runoff are the main sources of phosphorus (P) inputs into freshwater bodies, being the main cause of eutrophication (Burkholder, 2000; Carpenter, 2005). At global scale, the accumulation of P in terrestrial and freshwater aquatic ecosystems is 75% greater than pre-industrial levels (Bennett et al., 2001). In-lake addition of adsorbents, with the main objective of reducing lake water P concentration, is a recommendable lake management tool when the external P load has been previously reduced or the diffuse P sources are dominant (Deppe and Benndorf, 2002; Cooke et al., 2005). A wide variety of P adsorbents with different physico-chemical characteristics are commercially available. Aluminum (Al), iron (Fe) and calcium (Ca) salts (Hupfer and Hilt, 2008), modified zeolites (Phoslock®, Bephos® and Aqual-P®) or Fe oxy-hydroxides (CFH-12®) are some examples of non-magnetic materials proposed for P adsorption in natural systems (Gibbs and Özkundakci, 2011; Zamparas et al., 2013; Copetti et al., 2016). An important downside of non-magnetic materials is that their effectiveness and longevity may depend on the physic-chemistry and the stability of the water column, ageing and crystallization of flocs or bioturbation, among others factors (Huser et al., 2016). Bare and coated magnetic nano/microparticles such as magnetite (Fe_3O_4) or zero valent Fe (ZVI) have been recently proposed for P removal from freshwater bodies (de Vicente et al., 2010a; Funes et al., 2017). The recovery of the P-loaded adsorbents by applying a magnetic separation gradient is the main novelty of using magnetic adsorbents. This implies a short contact time of the adsorbent with biota, cost savings when reusing it and the possibility of recovering P for further use as potential fertilizer, which is a challenge that deserves attention given the future scarcity of rock P reserves (Cordell et al., 2009).

Apart from the physic-chemical characteristics of the adsorbent (e.g. particle size, specific surface area, surface charge, surface functional groups and dosage), environmental conditions (e.g. pH, ionic strength and competitive ions) play an important role in the P removal efficiency (Li et al., 2016). Berkowitz et al. (2005) reported a high affinity of reactive silicate (Si) for Al. The potential interference of Si and humic acids in the adsorption of P by Al hydroxide (de Vicente et al., 2008) and Fe oxy-hydroxides (goethite) (Sigg and Stumm, 1981; Antelo et al., 2007) has been previously suggested. Humic substances also interfere with the P adsorption on Phoslock® (Lürling et al., 2014; Dithmer et al., 2016) and present high affinity for the adsorption on magnetite surface (Illés and Tombácz, 2004). Reitzel et al. (2013) found a negative correlation between P adsorption capacity of Phoslock® and alkalinity. Apart from Dissolved Organic Carbon (DOC) and Si, major cations (Mg^{2+}, Na^{+}, K^{+}) and anions (SO_4^{2-}, Cl^{-}) are negatively related to P removal by ZVI magnetic microparticles (grade HQ; hereafter FeHQ) (de Vicente et al., 2011). Funes et al. (2017) also reported a reduction in DOC and Si concentration when applying the same magnetic particles (FeHQ) to microcosms containing lake water and surface sediment from a hypertrophic lake. The high affinity of heavy metals for bentonite, Fe_3O_4, Fe oxides and ZVI magnetic particles is widely documented in the literature (Veli and Alyüz, 2007; Feng et al., 2012; Hua et al., 2012; Funes et al., 2014).

The majority of laboratory P adsorption studies are focused on determining P removal efficiency in different matrices (i.e. Auvray et al., 2006; de Vicente et al., 2010a). Actually, the number of studies that assess the effect of interfering substances on the removal process by carrying out, either single-ion experiments (Borggaard et al., 2005; de Vicente et al., 2008; Merino-Martos et al., 2015), or adsorption experiments with natural lake water (de Vicente et al., 2008; de Vicente et al., 2011; Reitzel et al., 2013)

is growing. Single-ion experiments aim at evaluating the individual effect of each substances/ions on the performance of the adsorbents to remove P. Given the simplicity of this approach (single factor), the simple linear regression has been previously applied to study the relationship between an independent variable and P removal (de Vicente et al., 2008, 2011). However, natural lake waters are complex matrices in which the P removal efficiency is finally controlled by the interactions between coexisting substances/ions, the adsorbate and the adsorbent. Up to now, the statistical approaches applied in experiments with lake water are correlation analysis (Reitzel et al., 2013), simple linear regression (de Vicente et al., 2011) and principal component analysis (de Vicente et al., 2008). Unfortunately, correlation analysis and simple linear regression do not allow to distinguish if each factor by itself is interfering on P removal or if it is a consequence of the high correlation with other factors. Instead, the linear mixed models (LMMs) approach would be more suitable in these complex systems although they have not been previously used in similar studies.

Mediterranean ponds are ecosystems characterized by a high catchment area to volume ratio (Álvarez-Cobelas et al., 2005). This circumstance causes that the effect of the human activities generated in its drainage basin is of greater influence than in temperate lakes. Therefore, this "diffuse pollution" is responsible for the high concentrations of nutrients, heavy metals, DOC and other ions in these Mediterranean shallow ecosystems (Smith, 2009). These high concentrations make that, in a context of lake restoration, it is crucial to evaluate the main drivers controlling P adsorption in natural lake waters. In this work, we hypothesize that the chemical composition of lake water would affect P removal efficiency by different P adsorbents. To test this hypothesis, in this manuscript we run laboratory experiments by using four different P adsorbents -two non-magnetic (CFH-12® and Phoslock®) and two magnetic [FeHQ and hydrous lanthanum (La) oxide

loaded silica-coated magnetite, hereafter**,** Fe-Si-La]- in water samples from 20 Mediterranean aquatic ecosystems at two adsorbent dosages. All these adsorbents have been previously used to efficiently remove P in laboratory/microcosms experiments (e.g. de Vicente et al., 2010a; Reitzel et al., 2013; Lyngsie et al., 2014; Lai et al., 2016; Funes et al., 2017) and, specifically Phoslock®, at field scale (e.g. Robb et al., 2003; Meis et al., 2012). Finally, our objective was to determine the major drivers (e.g. humic substances, Si, major cations/anions) affecting P removal efficiency when using the above mentioned adsorbents by using linear mixed models.

2. MATERIALS AND METHODS

2.1 Sampling and chemical analysis of lake water

In March 2017, water samples with different chemical composition (Table 1) were collected from 20 inland aquatic ecosystems in southern Spain (see supplementary information SI Fig. S1). Once in the laboratory, pH and conductivity were measured with a pH meter (pH 196, WTW, Germany) and a conductivity meter (InoLab Con Level 1, WTW, Germany), respectively. Water samples were filtered through glass microfiber filters (GF/F, 0.7 μm) and the dissolved reactive P (Murphy and Riley, 1962), total dissolved Fe (Fe^{2+} and Fe^{3+}; Gibbs, 1979), Si (APHA, 1995) and color were spectrophotometrically analysed (Biochrom Libra S50). Color was determined at 440 nm in 1-cm cuvettes. Water color was expressed as absorption coefficient (a_{440}) in units of inverse meters (m^{-1}) according to the following equation (Reche and Pace, 2002):

$$a_{440} = \frac{2.303\ A440}{Z}$$

where $A440$ is the measured absorbance at 440 nm and Z is the optical path length (in m). Lake water used for measuring major cations [sodium (Na^+), potassium (K^+),

magnesium (Mg^{2+}) and calcium (Ca^{2+})], major anions [nitrates (NO_3^-), sulphates (SO_4^{2-}) and chlorides (Cl^-)] and heavy metals [manganese (Mn^{2+}), arsenic (As^{2-}), copper (Cu^{2+}) and nickel (Ni^{2+})] was filtered through Millipore 0.22 µm filters. Major cations and anions were measured by Ion Cromatography (IC; 940 Professional IC Vario, Metrohm) and heavy metals were analysed by inductively coupled plasma-mass spectroscopy (ICP-MS; Perkin Elmer NexION 300D). All physic-chemical parameters above mentioned were measured in the water samples four times along the experiment (six weeks): once at the beginning, twice during the experiment and the last one at the end of the experiment. Salinity of the systems was estimated by using conductivity measurements and the equation proposed by Alcorlo et al. (1996) for lakes located in the Guadalquivir Depression in southern Spain [salinity (g L^{-1}) = 0.8211 conductivity (mS cm^{-1}) = 0.18389]. Finally, DOC concentration was estimated from the relationship between DOC (measured with a Shimadzu TOC analyzer) and color (expressed as absorption coefficient, a_{440}; r^2 = 0.61; de Vicente et al., 2010b).

2.2 Synthesis of hydrous lanthanum oxide loaded silica-coated magnetite (Fe-Si-La)

Fe-Si-La particles were synthesized following the procedure of Lai et al. (2016) with slight modifications. Briefly, 10 g of commercial bare Fe_3O_4 (Sigma Aldrich; 50-100 nm) was dispersed in a mixture of ethanol (1.6 mL) and distilled water (400 mL). The suspension was horizontally shaked for 10 min at 200 rpm. Afterwards, 100 mL of ammonia (28%) and 3.26 mL of tetraethyloxysilane (TEOS, 98.6%) were added to the suspension and left for shaking for 6 h at 200 rpm. The Si coated Fe_3O_4 was magnetically separated and the supernatant was removed. Then, 500 mL of $LaCl_3$ (0.02 M) was added to the Si coated Fe_3O_4 and the pH of the suspension was raised to 10 by

adding 3M NaOH. After magnetic separation for 5 min, the Fe-Si-La particles were washed twice with distilled water, twice with absolute ethanol and the last time with acetone. In each washing step, the particles were sonicated for 15 min. Then, particles were air dried and stored at 4 ºC until used.

2.3 Characterization of the adsorbents

CFH-12® (Kemira, Finland) is a dry, granular and amorphous ferric oxy-hydroxide with a Fe content of ~ 44% w/w. As specified by the manufacturer (CSIRO, Australia), Phoslock® is a dry and granular compound consisting of La-modified clay (~ 5 % ww La). To obtain a homogenized fine powder (~250 nm), CFH-12® and Phoslock® were crushed in a mortar.

Fe-Si-La and commercial bare Fe_3O_4 particles were characterized with the following techniques. Surface morphology and particle size were determined by focus ion beam field-emission scanning electron microscopy (FIB-FESEM, AURIGA, Carl Zeiss SMT Inc.). A SQUID magnetometer (Quantum Design MPMS XL) was used to determine the magnetization curves of the powders at 293 K. Quantitative chemical composition of the surface was determined by X-ray photoelectron spectroscopy (XPS; Kratos Axis Ultra-DLD) with monochromatic Al Kα radiation. The wide spectrum (pass energy 160 eV) and spectra of the detected elements (pass energy 20 eV) were obtained using an electrostatic lens. The La content in Fe-Si-La was analysed by inductively coupled plasma-mass spectroscopy (ICP-MS; Perkin Elmer NexION 300D) following sample digestion with HNO_3 + HF.

FeHQ magnetic particles were supplied by BASF (Germany). According to the manufacturer, the composition of this powder is 97.5% iron, 0.9% carbon, 0.5%

oxygen, and 0.9% nitrogen. These particles are spherical in shape with an average diameter of 800 nm [see de Vicente et al. (2010a) for further characterization details].

2.4 Adsorption isotherms

The adsorption isotherms of the four adsorbents were conducted at room temperature (25 ºC) using the batch technique. The stock magnetic suspensions (50 g L^{-1}) were prepared by adding 2.5 grams of Fe-Si-La or FeHQ in a final volume of 50 mL. Prior to their use, stock magnetic suspensions were sonicated for 5 min. A volume of 1 mL of the stock magnetic suspensions was mixed with 40 mL of 3 mM $NaHCO_3$ in a polyethylene container and agitated for 24 h at 150 rpm. In the case of non-magnetic adsorbents (CFH-12® and Phoslock®), 0.05 g were added as dry material to polyethylene containers along with 40 mL of 3mM $NaHCO_3$ and agitated under the same conditions. 1 mL of different P stock solutions ranging from 5 to 60 mM P was added to the containers and the pH was adjusted to 7. Suspensions were agitated again for 24 h at 150 rpm. After 24 h of agitation, pH was readjusted to 7 and suspensions were made up to 50 mL to give final P concentrations ranging from 0.1 mM to 1.2 mM. The final adsorbent concentration in the adsorption experiments was 1 g L^{-1} for all the adsorbents. Adsorbents were then separated from the supernatant by centrifugation (10 min, 3000 rpm) or using a variable gap magnet (5 min; PASCO scientific; EM-8641). Supernatant was filtered through glass microfiber filters (GF/F, 0.7 µm) and dissolved reactive P was spectrophotometrically determined (Murphy and Riley, 1962). The equilibrium adsorption capacity was calculated as follows:

$$q = \frac{C_{cont} - C_e}{M_a} V \qquad [1]$$

being C_{cont} the P concentration in the control treatment, that is, the P concentration in lake water 24 h after the addition of P and without adsorbent; C_e the equilibrium P

concentration (mg L^{-1}); M_a the mass of adsorbent (g) and V the total volume of the suspension (L). C_{cont} was different across the lakes. We used C_{cont} to calculate q instead of the starting P concentration (20 µM) to avoid including the interaction of P with water chemistry in the calculation.

2.5 Adsorption experiments with lake water

The standard suspensions (25 g L^{-1}) of magnetic adsorbents (Fe-Si-La and FeHQ) were prepared as follows: (i) 625 mg of magnetic adsorbent were mixed with distilled water in a polypropylene container (25 mL); (ii) To ensure homogeneity of the sample, the suspension was sonicated for 5 min prior to its use in the adsorption experiments. A standard solution of 5 mM P was prepared by adding 136 mg of KH_2PO_4 to distilled water (200 mL).

For the batch adsorption experiments, nine different treatments were applied in which four adsorbents -CFH-12®, Phoslock®, Fe-Si-La and FeHQ- were tested at two dosages and one treatment, with no adsorbent addition, served as control. Each treatment was performed with six replicates, measuring one replicate of each treatment per week (six weeks in total). Depending on the P concentration measured in water samples, different volumes of a standard solution (5 mM P) were added to obtain a fixed concentration of 20 µM P in all systems in a volume of 25 mL. The adsorbents were then added to 25 mL of lake water as follows: 3.3 and 7.8 mg of non magnetic adsorbents (CFH-12® and Phoslock®) were weighed and added to the lake water in order to test a low and high adsorbent:P ratio, respectively, for each adsorbent. The magnetic adsorbents (Fe-Si-La and FeHQ) were added as suspensions by using a volume of 124 or 310 µL from the standard magnetic suspension (25 g L^{-1}) to obtain the low and high adsorbent:P ratio, respectively. Samples were then agitated for 20 h in a horizontal shaker (150 rpm).

After this time, the supernatant was separated from the adsorbents by centrifugation (3 min, 3000 rpm) or by using the variable gap magnet for 1 min (PASCO scientific; EM-8641). Finally, the supernatant was filtered for dissolved reactive P analysis (C_e). P removal efficiency (Pr, %) was calculated as follows:

$$\mathrm{Pr} = \frac{C_{cont} - C_e}{C_{cont}} 100 \quad [2]$$

Likewise, adsorbed P (µmol) was calculated as (C_{cont}-C_e)V [3], where the terms in both equations are the same as in equation but here the units of C_{cont} and C_e are µmol L^{-1}[1]. The adsorbent dosages (low and high) were established according to the adsorption isotherms represented in Fig. 1. As seen in Fig. 1, P adsorption capacity of the four adsorbents ranges between 1.6 and 2.6 mg P g^{-1} adsorbent (adsorbent:P ratio of 0.38 g mg^{-1}) when testing them at P concentrations below 0.1 mM (which is a more similar concentration to eutrophicated waters). Accordingly, a lower (0.2 g mg^{-1}) and a higher (0.5 g mg^{-1}) adsorbent:P ratio were tested in order to study the effect of adsorbent dosage on P removal efficiency.

2.6 Data analysis

The aim of the statistical analysis was to identify major factors affecting P removal efficiency by different adsorbents. A LMM was performed considering the *replicates* and the *lakes* (location) as random factors. In consequence, *replicates* and *lakes* are considered a random sample of all possible replicates and all possible lakes, respectively. The adsorbed P data were power-transformed (x^2) prior to analysis to meet the assumption of normality of residuals. The absence of outliers and multicollinearity (*vif* function) were fulfilled. At the initial stage, the variables studied were selected according to the following criteria: (1) potential interference of the variable in P removal according to the literature (see introduction) and (2) high enough

value/concentration to cause interferences. The variables initially studied were: type of adsorbent, adsorbent dosage, conductivity, major cations and anions, pH, color, Si, heavy metals (Mn^{2+}, As^{2-}, Cu^{2+} and Ni^{2+}) and C_{cont}. Aiming at avoiding redundancy between independent variables, Spearman's correlation test with the Holm´s correction was firstly accomplished. As a result, major cations, major anions and *Ni* were not included in the global model due to their high correlation with conductivity (Na^{+} r = 0.70; K^{+} r = 0.92; Mg^{2+} r = 0.92; Ca^{2+} r = 0.96; Cl^{-} r = 0.96; SO_4^{2-} r = 0.82; Ni^{2+} r = 0.73; p values for all correlations < 0.0001). A global model containing the factors (1) type of adsorbent, (2) adsorbent dosage, (3) conductivity, (4) pH, (5) color, (6) Si, (7) NO_3^{-}, (8) Mn^{2+}, (9) As^{2-} and (10) Cu^{2+} and (11) C_{cont} (P in lake water after 24 h without adsorbent) was finally analysed by using lme4 package (Bates et al., 2015). Model selection was conducted using MuMIn package (Bartoń, 2012). The Akaike information criterion (AIC*c*) values allow to establish a ranking of candidate models. Models with a ΔAIC_c (differences in AIC_c values of the model and the model with the smallest AIC_c) less than 2 were given similar support (Posada and Buckley, 2004). The best model was the model with the minimum AIC_c value showing a difference higher than 2 AIC_c units with other models (Burnham and Anderson, 1998; Posada and Buckley, 2004). A final model including all variables retained in the selected models was performed. The Tukey's post hoc test was done with multcomp package (Hothorn et al., 2013). The significant interactions between factors were studied by testing the simple main effects and performing contrasts across the levels of one factor when the values for other factors are fixed at a certain level with phia package (de Rosario-Martínez, 2015). We also tested the contribution of random effects using the likelihood ratio test (Bolker et al. 2009). The model analyses were performed in R software (R Development Core Team, 2017). Significant differences were considered when $p < 0.05$.

3. RESULTS AND DISCUSSION

3.1 Characterization of hydrous lanthanum oxide loaded silica-coated magnetite (Fe-Si-La)

A SEM image of the Fe-Si-La particles is shown in Fig. 2. As observed, particles are quasi-spherical in shape and polydisperse in size with a mean particle size of ~100 nm. Fig. 3 shows the magnetic hysteresis curve of commercial bare Fe_3O_4 and Fe-Si-La particles at 293 K. Both particles behave as soft magnetic materials with negligible coercitive field and remnant magnetization, which means that magnetization becomes zero when removing the field. The saturation magnetization (*Ms*) of Fe-Si-La (81 emu g^{-1}) is slightly lower than bare Fe_3O_4 (89 emu g^{-1}) due to the presence of the non-magnetic inorganic coating. Table 2 shows their surface chemical composition as obtained by XPS. This analysis evidenced a significant presence of Si (13.0%) and La (5.3%) at the surface of the Fe-Si-La particles. The lower bulk La content in Fe-Si-La (0.9%) determined by ICP-MS demonstrates that La is mainly located on the particle surface.

3.2 Maximum phosphorus adsorption capacity of the adsorbents

P adsorption capacity of CFH-12®, Phoslock® and Fe-Si-La (also bare commercial Fe_3O_4 is studied) were assessed by modelling the adsorption data. Experimental data were fit to Langmuir and Dubinin–Radushkevich (DR) adsorption isotherms (see solid lines in Fig. 1). Langmuir isotherm model assumes a homogeneous adsorption surface in which a monolayer of adsorbate is formed and is defined by the equation [4]:

$$q_e = \frac{K_L M_L C_e}{1+K_L C_e} \quad [4]$$

where q_e is the amount of adsorbed adsorbate at equilibrium (mg g^{-1}), K_L (L g^{-1}) is an adsorption constant related to the energy of adsorption, M_L (mg g^{-1}) is an empirical saturation constant that represents the maximum adsorption capacity and C_e is the same as in equation [1]. The DR equation is widely used to describe the pore filling adsorption mechanism on microporous surfaces such as activated carbon, zeolites and clays and it is represented by the equations [5] and [6] (Nguyen and Do, 2001; Brezovska et al., 2004; Chen, 2015):

$$q_e = q_s \, exp(-K_{DR} \varepsilon^2) \quad [5]$$

$$\varepsilon = RT \, ln \, (1 + \frac{1}{c_e}) \quad [6]$$

where q_s (mg P g^{-1}) is a constant representing the maximum adsorption capacity, K_{DR} (mol^2 kJ^{-2}) is a constant related to the free energy of adsorption, R is the universal gas constant (8.314 J mol^{-1} K^{-1}) and T (K) is the absolute temperature. Attending to r^2 values, Phoslock® (a modified bentonite) showed a better fit to DR isotherm. These results were expected as bentonite is a microporous material (Brezovska et al., 2004) and accordingly, the adsorption process is well explained by the pore filling mechanism described by DR isotherm. In contrast, CFH-12® and Fe-Si-La (also Fe_3O_4) fit better to Langmuir isotherm (SI Table S1). Comparison of the four adsorbents evidenced that FeHQ had the highest adsorption capacity (18.8 mg g^{-1}; see de Vicente et al., 2010a), followed by CFH-12® (15.1 mg g^{-1}), Phoslock® (13.6 mg g^{-1}) and Fe-Si-La (6.7 mg g^{-1}). As seen, Fe-Si-La showed higher adsorption capacity compared to bare Fe_3O_4 (5.85 mg g^{-1}). In general, similar values were obtained in previous works for the same adsorbents. The manufacturer reported a M_L of 10.0 mg P g^{-1} for Phoslock® (CSIRO, Australia). Fuchs et al. (2018) obtained a M_L of 30.6 mg P g^{-1} for CFH-12® which is twice the value of this work presumably due to longer contact time [3 months of exposure to 50

μM of dissolved inorganic P (DIP)]. However, the maximum P adsorption capacity of our Fe-Si-La particles was much lower than that reported by Lai et al. (2016) with similar particles (27.8 mg g^{-1}). This discrepancy may arise from differences in the preparation method. In fact, a much lower La content is present in our Fe-Si-La particles as indicated by ICP-MS (0.9% total La) and by XPS (5.3% of surface La content) compared to Lai et al. (2016).

3.3 Factors affecting phosphorus adsorption

According to the AIC_c values and the Akaike weights (ω, conditional probabilities of each model) of the models, three models received noticeable support and were considered plausible to identify factors controlling P adsorption (Table 3). Model A had the smallest AIC_c value (best model) and contained as independent variables: type of adsorbent, adsorbent dosage, their interaction term (type of adsorbent x adsorbent dosage) and C_{cont}. Additionally to the variables present in model A, model B included NO_3^- concentration and the interaction NO_3^- x type of adsorbent whereas model C added color as independent variables. As a result, a final model containing all the variables present in the three selected models was obtained. Results of the LMM are shown in Table 4. As seen, all parameters except for NO_3^- (type of adsorbent, adsorbent dosage, color and C_{cont}) and the interactions included in the model had a significant effect ($p < 0.05$) on P adsorption. In the following sections the effect of each parameter is studied in detail.

Results showed that none of the random factors showed a significant effect on P adsorption (replicate: $p = 0.813$; lake: $p = 1$). These results allow us to extrapolate the results obtained in the model to other lakes.

3.3.1 Effect of the type of adsorbent

As seen in Table 4, the type of adsorbent had a significant effect on P adsorption. P removal efficiencies at low and high adsorbent dosage are represented for all the adsorbents in Fig. 4. Data represent the average for all aquatic ecosystems. As expected, those adsorbents with the highest maximum P adsorption capacities, CFH-12® and Phoslock® (SI Table S1), showed the highest P removal efficiencies (> 85%). Fe-Si-La was also very efficient with P removal efficiencies greater than 70% whereas FeHQ showed the lowest (≤ 15%). Tukey's post hoc test (data not shown) showed that Phoslock® removed significantly more P than CFH-12®, Fe-Si-La and FeHQ ($p = 0.037$, $p = 0.01$, $p < 0.001$, respectively). P removal was significantly lower for FeHQ compared to the rest of the adsorbents ($p < 0.001$). This result is especially striking in view of the high maximum P adsorption capacity of FeHQ (de Vicente et al., 2010a); however different explanations can be suggested. First, the low adsorption capacity of FeHQ (0.5 mg g^{-1}; de Vicente et al., 2010a) at low P concentrations (< 0.1 mM P) compared to the rest of the adsorbents (1.6-2.5 mg g^{-1}; see Fig. 1). Second, the adsorbent:P ratios used in this work (0.2 and 0.5 g mg^{-1}) are seven and three fold lower, respectively, than the optimum adsorbent dosage (1.5 g mg^{-1}) calculated by Merino-Martos et al. (2011) to efficiently remove P from solution. Even more, de Vicente et al. (2011) applied much higher adsorbent dosages (6.45 and 25.81 g mg^{-1}) when using the same particles to remove P from different natural aquatic ecosystems. Given the low P removal by FeHQ, a complementary model was run in which FeHQ was removed, determining that the type of adsorbent was not significant ($p = 0.793$) for the overall model (data not shown). In this case, differences between the three other adsorbents are not relevant as determined by Tukey's test ($p = 0.622$, $p = 0.514$, $p = 0.877$).

3.3.2 Effect of the adsorbent dosage

The adsorbent dosage is, as expected, a significant factor explaining the mass of adsorbed P (Table 4). As seen in Fig. 4, the high adsorbent dosage led to higher P removal efficiencies. Likewise, there is an interactive effect of the factors type of adsorbent x adsorbent dosage on adsorbed P (Table 4). As a result, a post hoc analysis of this interaction was carried out. Table 5 shows the results of simple main effects interaction analysis for type of adsorbent x adsorbent dosage. In consequence, the effect of adsorbent dosage at the different types of adsorbents was tested, and it was found that the adsorbent dosage has a significant effect on adsorbed P ($p < 0.001$) when using CFH-12® and Fe-Si-La but not when using Phoslock® and FeHQ ($p > 0.05$). Specifically, when comparing adsorbent dosages for CFH-12® (Fig. 4), we observed that the high adsorbent dosage removed significantly more P (> 99% on average for all the systems) than the low adsorbent dosage (86.1%). Similarly, when adding Fe-Si-La P removal efficiencies were significantly higher for the high dosage (> 99%) than for the low dosage (71.2%; Fig. 4). However, no differences in adsorbed P were found between the high and low adsorbent dosage for the case of Phoslock® (97.5-99.1%) and FeHQ (12.0-15.5%). Differences in the effect of adsorbent dosage on adsorbed P among the studied adsorbents explain the significant interaction between the factors type of adsorbent x adsorbent dosage obtained in the model.

3.3.3 Effect of the matrix

Among all the variables included in the model, C_{cont} and color in lake water were the only ones related to water chemical composition that significantly affect adsorbed P (Table 4). On the one hand, the coefficient for C_{cont} is positive, pointing out a positive relationship between C_{cont} and the mass of adsorbed P. In particular, Phoslock® showed

the strongest Pearson correlation coefficient (r = 0.940) between C_{cont} and P adsorbed followed by CFH-12® (r = 0.731) and Fe-Si-La (r = 0.428). Therefore, high C_{cont} would enhance the mass of adsorbed P. This trend has been also observed for anionic dyes (Banerjee and Chattopadhyaya, 2017). By contrast, a negative and weak correlation (r = -0.060) between both variables were found for FeHQ as a result of the insufficient adsorbent dosage. On the other hand, the coefficient for color was negative, reflecting that the mass of adsorbed P responded inversely to increasing values of this parameter. Color in water has been reported to be a good indicator of the humic substances (humic and fulvic acids) concentration (Cuthbert and del Giorgio, 1992). In more details, Fig. 5 shows the relationship between adsorbed P and color for all the adsorbents. As indicated by r values, high values of color and thus, high lake water concentrations of humic substances, would noticeably affect the mass of adsorbed P by Fe-Si-La (r = -0.164) and by CFH-12® (r = -0.109). Previous works have reported potential interferences of humic acids on the adsorption of P onto Fe oxy-hydroxides, a similar Fe based compound to CFH-12® (Antelo et al., 2007) and onto Fe-Si-La (Lai et al., 2016). Humic substances may interact with colloids in different ways. H-bonding, ligand exchange and electrostatic interactions are the main sorption mechanisms of humic substances onto iron oxides (goethite and hematite) (Philippe and Schaumann, 2014). Frequently, several mechanisms act at the same time. The humic substances that mostly affect P adsorption onto iron oxides are fulvic acids due to a stronger electrostatic interactions with P (Weng et al., 2008).

Unlike what happened to CFH-12® and Fe-Si-La, humic substances had negligible effect on adsorbed P by Phoslock® (r = -0.042) despite the fact that the DOC concentration in the studied aquatic systems were high enough to cause interferences (Lurling et al., 2014; Dithmer et al., 2016). Specifically, half of the lakes presented a

DOC concentrations between 1 to 10 mg L^{-1} and half presented values ranging from 10 to 30 mg L^{-1} except for Charca Suárez which showed much higher value (118 mg DOC L^{-1}). Contrarily to our results, the competition of humic substances and P for the adsorption sites on Phoslock® has been previously reported (Dithmer et al., 2016). Similarly, Lurling et al. (2014) reported a reduced P binding by Phoslock (actually by La which is the active ingredient) when DOC concentrations were as low as 2 mg L^{-1} and the effect became stronger when increasing up to 14 mg DOC L^{-1}. The stronger effect of humic substances on P adsorption by CFH-12® and Fe-La-Si than by Phoslock® may be explained by several reasons. Firstly, the high adsorption capacity of Phoslock® compared to the others adsorbents (see SI Table S1). According to the results, P removal by Phoslock® was not affected by coexisting ions and substances (almost 100% of P removal whatever the adsorbent dosage and lake water) because there are still free adsorption sites for P. However, in Fe-Si-La and CFH-12®, the adsorption sites (OH functional groups) could be blocked by the presence of humic substances and not available for P adsorption, thus reducing P removal efficiency (Lai et al., 2016; Borggaard et al., 2005). A second explanation would be the lower affinity of humic substances for clays compared to iron oxides due to the unfavourable electrostatic pattern (Philippe and Schaumann, 2014). Another reason maybe that the adsorption of humic substances on CFH-12® and on Fe-Si-La could reduce their point of zero charge (pzc) and increase electrostatic repulsion for the adsorption of anionic phosphate (Antelo et al., 2007).

As seen in Table 4, there are not significant main effects of NO_3^- on the adsorbed P. However, there is a significant effect of the interaction type of adsorbent x NO_3^-. This means that the effect of NO_3^- on the adsorbed P depends on the type of adsorbent. Table 6 shows the post hoc analysis of this interaction in which the adjusted values of the

slope with respect to the adsorbed P for the level and contrasts of the type of adsorbent are indicated. According to it, the proportional relation between NO_3^- and adsorbed P is significantly greater (and direct, see Fig. 6) for FeHQ compared to the rest of adsorbents ($p < 0.001$). Likewise, this proportional relation is significantly different (and negative, see Fig. 6) for Phoslock® compared to CFH-12® and Fe-Si-La ($p < 0.05$ and $p < 0.01$, respectively). In fact, Table 7 points out that the relation between adsorbed P and NO_3^- is only significant for FeHQ and Phoslock®. This result may have implications in lake restoration. The efficiency of Phoslock in removing P could be reduced in lakes with high NO_3^- concentration whereas the efficiency of FeHQ would increase. Pr in each aquatic ecosystem is shown in Fig. 7 and Fig. 8 for non-magnetic and magnetic adsorbents, respectively. For CFH-12®, Pr was similar between lakes at low adsorbent dosage. At high adsorbent dosage of CFH-12®, Charca Suárez showed the lowest Pr (94.2%) compared to the highest value found in Grande, Padul and Cubillas (99%). For Phoslock® and Fe-Si-La, Pr was similar across lakes at high adsorbent dosage but the values were different at low adsorbent dosage. Pr by Phoslock® was slightly lower in Charca Suárez (81.3%) compared to Balax (99.9%). Pr by Fe-Si-La was notably lower in Charca Suárez (38.3%) and Canales (63.0%) compared to Colomera (82.6%), Cubillas (89.5%) and Guadalén (80.0%). For the case of FeHQ, Pr was similar between lakes at low adsorbent dosage whereas it was different at high adsorbent dosage, being Pr much lower in Puerto de los Alazores (5.3%) compared to Balax (49.0%).

The lower Pr reported in Charca Suárez for all the adsorbents could be attributed to its extremely high color value (10.31 m^{-1}), which ultimately reflects high humic substances concentration (Cuthbert and del Giorgio, 1992). Similarly, and although As was not selected in the model as explanatory variable for P adsorption, the high concentration of this metal in Charca Suárez (11.7 µg L^{-1}) may have reduced adsorbed P by CFH-12®

due to competition. In fact, P and As have been reported to have a similar structure, chemical reactivity and adsorption kinetic onto iron oxides (Luengo et al., 2007; Lukkari et al., 2007).

4. Conclusions

For the practical application of novel P adsorbents used for lake restoration, it is essential to assess the effects that natural substances/ions have on P removal efficiency. In this study, adsorption experimental data from 20 aquatic ecosystems, have been used for obtaining a linear mixed model. This novel methodological approach has determined that the major drivers controlling P removal are: type of adsorbent, the adsorbent dosage and the concentration of humic substances. The studied adsorbents showed the following P removal efficiency order: Phoslock® (~100%) > CFH-12® (85-100%) > Fe-Si-La (70-100%) > FeHQ (0-15%) for both adsorbent:P ratios 0.2 and 0.5 g mg^{-1}. Phoslock® was the most efficient P adsorbent independently of adsorbent dosage and water chemical composition. Contrarily to previous studies, FeHQ showed a low P uptake due to a notable underdosing. P removal efficiency of CFH-12® and Fe-Si-La was negatively affected by high color values (high humic substances). With regards to the P removal efficiency, the non-magnetic adsorbents employed in this work were more efficient than their magnetic counterparts. However, it is important to remark that the former cannot be reused. All in all, differences in chemical properties -adsorption capacity or surface charge- and the affinity to the adsorbate and to other substances/ions play an important role in the performance of each adsorbent to remove P.

5. Acknowledgments

This work was supported by Junta de Andalucía project P10-RNM-6630 [Proyectos de Excelencia, Spain]; MINECO CTM 2013-46951-R project; and MAT 2016-78778-R project [Spain]. Authors would also like to thank Fernando Ortega for helping in the sampling procedure.

6. References

Alcorlo, P., Baltanás, A., Montes, C., 1996. Is it possible to predict the salinity of Iberian salt lakes from their conductivity ? Hydrobiologia 330, 137–142.

Álvarez-Cobelas, M., Rojo, C., Angeler, D.G., 2005. Mediterranean limnology: current status, gaps and the future. Journal of Limnology 64, 13-29. doi.org/10.4081/jlimnol.2005.13

Antelo, J., Arce, F., Avena, M., Fiol, S., López, R., Macías, F., 2007. Adsorption of a soil humic acid at the surface of goethite and its competitive interaction with phosphate. Geoderma 138, 12–19. doi:10.1016/j.geoderma.2006.10.011

APHA, 1995. Standard Methods for Examination of Water and Wastewater. 19th ed. APHA-AWWA-WPCF, Washington, DC, USA.

Auvray, F., van Hullebusch, E.D., Deluchat, V., Baudu, M., 2006. Laboratory investigation of the phosphorus removal (SRP and TP) from eutrophic lake water treated with aluminium. Water Res. 40, 2713–2719. doi:10.1016/j.watres.2006.04.042

Banerjee, S., Chattopadhyaya, M.C., 2017. Adsorption characteristics for the removal of a toxic dye , tartrazine from aqueous solutions by a low cost agricultural by-product. Arab. J. Chem. 10, S1629–S1638. doi:10.1016/j.arabjc.2013.06.005

Bartoń, K., 2012. MuMIn: Multi-model inference. R package version 1.7.2. http://CRAN.R-project.org/package=MuMIn

Bates, D., Mächler, M., Bolker, B., Walker, S., 2015. Fitting linear mixed-effects

models using lme4. J. Stat. Soft. 67, 1–48. doi:10.18637/jss.v067.i01

Bennett, E.M., Carpenter, S.R., Caraco, N.F., 2001. Human Impact on Erodable Phosphorus and Eutrophication : A Global Perspective. BioScience 51, 227–234.

Berkowitz, J., Anderson, M. A., Graham, R.C., 2005. Laboratory investigation of aluminum solubility and solid-phase properties following alum treatment of lake waters. Water Res. 39, 3918–3928. doi:10.1016/j.watres.2005.06.025

Bolker, B. M., Brooks, M. E., Clark, C. J., Geange, S. W., Poulsen, J. R., Stevens, M. H. H., White, J. S. S., 2009. Generalized linear mixed models: a practical guide for ecology and evolution. Trends Ecol. Evol. 24, 127-135.

Borggaard, O.K., Raben-Lange, B., Gimsing, A.L., Strobel, B.W., 2005. Influence of humic substances on phosphate adsorption by aluminium and iron oxides. Geoderma 127, 270–279. doi:10.1016/j.geoderma.2004.12.011

Brezovska, S., Marina, B., Panova, B., Burevski, D., Bosevska, V., Stojanovska, L., 2004. The adsorption characteristics and porous structure of bentonite adsorbents as determined from the adsorption isotherms of benzene vapor. J.Serb.Chem.Soic. 69, 145–151.

Burkholder, J. M. 2000. Eutrophication and oligotrophication, p. 649–670. *In* S. Levin (ed.), Encyclop. Biodivers. Volume 2. Academic Press, New York.

Burnham, K. P., Anderson, D. R., 1998. Model selection and inference. A Practical information-theoretic approach. 2nd edition. New York: Springer.

Carpenter, S.R., 2005. Eutrophication of aquatic ecosystems: bistability and soil phosphorus. Proc. Natl. Acad. Sci. U. S. A. 102, 10002–10005. doi:10.1073/pnas.0503959102

Chen, X., 2015. Modeling of experimental adsorption isotherm data. Information 6, 14–22. doi:10.3390/info6010014

Cooke, G.D., Welch, E.B., Peterson, S.A., Nichols, S.A., 2005. Restoration and Management of Lakes and Reservoirs, third ed. CRC Press, Boca Raton, FL, p. 548.

Copetti, D., Finsterle, K., Marziali, L., Stefani, F., Tartari, G., Douglas, G., Reitzel, K., Spears, B.M., Winfield, I.J., Crosa, G., D'Haese, P., Yasseri, S., Lürling, M., 2016. Eutrophication management in surface waters using lanthanum modified bentonite: a review. Water Res. 97, 162-174. doi:10.1016/j.watres.2015.11.056

Cordell, D., Drangert, J.O., White, S., 2009. The story of phosphorus: Global food security and food for thought. Glob. Environ. Chang. 19, 292–305. doi:10.1016/j.gloenvcha.2008.10.009

Cuthbert, I. D., del Giorgio, P., 1992. Towards a standard method of measuring color in freshwater. Limnol. Oceanogr. 37, 1319–1326.

de Rosario-Martínez, HDR (2015). Analysing interactions of fitted models. https://cran.r-project.org/web/packages/phia/vignettes/phia.pdf

de Vicente, I., Jensen, H.S., Andersen, F.Ø., 2008. Factors affecting phosphate adsorption to aluminum in lake water: Implications for lake restoration. Sci. Total Environ. 389, 29–36. doi:10.1016/j.scitotenv.2007.08.040

de Vicente, I., Merino-Martos, A., Cruz-Pizarro, L., de Vicente, J., 2010a. On the use of magnetic nano and microparticles for lake restoration. J. Hazard. Mater. 181, 375–381. doi:10.1016/j.jhazmat.2010.05.020

de Vicente, I., Ortega-Retuerta, E., Mazuecos, I., Pace, M., Cole, J., Reche, I., 2010b. Variation in transparent exopolymer particles in relation to biological and chemical factors in two contrasting lake districts. Aquat. Sci. 72, 443–453 443–453. doi:10.1007/s00027-010-0147-6

de Vicente, I., Merino-Martos, A., Guerrero, F., Amores, V., de Vicente, J., 2011.

Chemical interferences when using high gradient magnetic separation for phosphate removal: Consequences for lake restoration. J. Hazard. Mater. 192, 995–1001. doi:10.1016/j.jhazmat.2011.05.090

Deppe, T., Benndorf, J., 2002. Phosphorus reduction in a shallow hypereutrophic reservoir by in-lake dosage of ferrous iron. Water Res. 36, 4525–4534. doi:10.1016/S0043-1354(02)00193-8

Dithmer, L., Nielsen, U.G., Lundberg, D., Reitzel, K., 2016. Influence of dissolved organic carbon on the efficiency of P sequestration by a lanthanum modified clay 97, 39–46. doi:10.1016/j.watres.2015.07.003

Feng, L., Cao, M., Ma, X., Zhu, Y., Hu, C., 2012. Superparamagnetic high-surface-area Fe_3O_4 nanoparticles as adsorbents for arsenic removal. J. Hazard. Mater. 217, 439–446.Funes, A., Arco, A., Álvarez-Manzaneda, I., de Vicente, J., de Vicente, I., 2017. A microcosm experiment to determine the consequences of magnetic microparticles application on water quality and sediment phosphorus pools. Sci. Total Environ. 579, 245–253. doi:10.1016/j.scitotenv.2016.11.120

Fuchs, E., Funes, A., Saar, K., Reitzel, K., Jensen, H.S., 2018. Evaluation of dried amorphous ferric hydroxide CFH-12® as agent for binding bioavailable phosphorus in lake sediments. Sci. Total Environ. 628–629, 990–996. doi:10.1016/j.scitotenv.2018.02.059

Funes, A., de Vicente, J., Cruz-Pizarro, L., de Vicente, I., 2014. The influence of pH on manganese removal by magnetic microparticles in solution. Water Res. 53, 110–122. doi:10.1016/j.watres.2014.01.029

Gibbs, M.M., 1979. A simple method for the rapid determination of iron in natural waters. Water Res. 13, 295–297. doi:10.1016/0043-1354(79)90209-4

Gibbs, M., Özkundakci, D., 2011. Effects of a modified zeolite on P and N processes

and fluxes across the lake sediment-water interface using core incubations. Hydrobiologia 661, 21–35. doi:10.1007/s10750-009-0071-8

Hothorn, T., Bretz, F., Westfall, P., Heiberger, R.M., Schuetzenmeister, A. 2013. Package "multcomp". http://cran.rproject.org/web/packages/multcomp/multcomp.pdf

Hua, M., Zhang, S., Pan, B., Zhang, W., Lv, L., Zhang, Q., 2012. Heavy metal removal from water/wastewater by nanosized metal oxides: a review. J. Hazard. Mater. 211, 317–331.

Hupfer, M., Hilt, S., 2008. Lake restoration. Encycl. Ecol. 2080–2093.

Huser, B.J., Egemose, S., Harper, H., Hupfer, M., Jensen, H., Pilgrim, K.M., Reitzel, K., Rydin, E., Futter, M., 2016. Longevity and effectiveness of aluminum addition to reduce sediment phosphorus release and restore lake water quality. Water Res. 97, 122–132. doi:10.1016/j.watres.2015.06.051

Illés, E., Tombácz, E., 2004. The role of variable surface charge and surface complexation in the adsorption of humic acid on magnetite. Colloids Surfaces A Physicochem. Eng. Asp. 230, 99–109. doi:10.1016/j.colsurfa.2003.09.017

Lai, L., Xie, Q., Chi, L., Gu, W., Wu, D., 2016. Adsorption of phosphate from water by easily separable Fe_3O_4@SiO_2 core/shell magnetic nanoparticles functionalized with hydrous lanthanum oxide. J. Colloid Interface Sci. 465, 76–82. doi:10.1016/j.jcis.2015.11.043

Li, M., Liu, J., Xu, Y., Qian, G., 2016. Phosphate adsorption on metal oxides and metal hydroxides : A comparative review. Environ. Rev. 24, 1–14. doi:10.1139/er-2015-0080

Luengo, C., Brigante, M., Avena, M., 2007. Adsorption kinetics of phosphate and arsenate on goethite. A comparative study 311, 354–360.

doi:10.1016/j.jcis.2007.03.027

Lukkari, K., Hartikainen, H., Leivuori, M., 2007. Fractionation of sediment phosphorus revisited. I : Fractionation steps and their biogeochemical basis. Limnol. Oceanogr. Methods 5, 433–444.

Lürling, M., Waajen, G., Van Oosterhout, F., 2014. Humic substances interfere with phosphate removal by lanthanum modified clay in controlling eutrophication. Water Res. 54, 78–88. doi:10.1016/j.watres.2014.01.059

Lyngsie, G., Borggaard, O.K., Hansen, H.C.B., 2014. A three-step test of phosphate sorption efficiency of potential agricultural drainage filter materials. Water Res. 51, 256–265. doi:10.1016/j.watres.2013.10.061

Meis, S., Spears, B.M., Maberly, S.C., O'Malley, M.B., Perkins, R.G., 2012. Sediment amendment with Phoslock® in Clatto Reservoir (Dundee, UK): Investigating changes in sediment elemental composition and phosphorus fractionation. J. Environ. Manage. 93, 185–193. doi:10.1016/j.jenvman.2011.09.015

Merino-Martos, A., de Vicente, J., Cruz-Pizarro, L., de Vicente, I., 2011. Setting up High Gradient Magnetic Separation for combating eutrophication of inland waters. J. Hazard. Mater. 186, 2068–2074. doi:10.1016/j.jhazmat.2010.12.118

Merino-Martos, A., de Vicente, J., Cruz-Pizarro, L., de Vicente, I., 2015. Single-ion interferences when using magnetic microparticles for phosphorus removal in aquatic ecosystems. Limnetica 34, 17–28.

Murphy, J., Riley, J.P., 1962. A modified single solution method for the determination of phosphate in natural waters. Anal. Chim. Acta 27, 31–36. doi:10.1016/S0003-2670(00)88444-5

Nguyen, C., Do, D.D., 2001. The Dubinin – Radushkevich equation and the underlying microscopic adsorption description. Carbon 39, 1327–1336.

Philippe, A., Schaumann, G.E., 2014. Interactions of dissolved organic matter with natural and engineered inorganic colloids : A Review. Environ. Sci. Technol. 48, 8946-8962. dx.doi.org/10.1021/es502342r

Posada, D., Buckley, T.R., 2004. Model selection and model averaging in phylogenetics: advantages of Akaike Information Criterion and bayesian approaches over likelihood ratio tests. Syst. Biol., 53, 793-808.

R Core Team, 2017. R: A language and environment for statistical computing. R Foundation for Statistical Computing, Vienna, Austria. https://www.R-project.org/.

Reche, I., Pace, M.L., 2002. Linking dynamics of dissolved organic carbon in a forested lake with environmental factors. Biogeochemistry 61, 21–36. doi:10.1023/A:1020234900383

Reitzel, K., Andersen, F.Ø., Egemose, S., Jensen, H.S., 2013. Phosphate adsorption by lanthanum modified bentonite clay in fresh and brackish water. Water Res. 47, 2787–2796. doi:10.1016/j.watres.2013.02.051

Robb, M., Greenop, B., Goss, Z., Douglas, G., Adeney, J., 2003. Application of Phoslock^{TM}, an innovative phosphorus binding clay, to two Western Australian waterways: Preliminary findings. Hydrobiologia 494, 237–243. http://doi.org/10.1023/A:1025478618611

Schindler, D.W., 2006. Recent advances in the understanding and management of eutrophication. Limnology and Oceanography 51, 356-363. 10.4319/lo.2006.51.1_part_2.0356

Sigg, L., Stumm, W., 1981. The interaction of anions and weak acids with the hydrous goethite (α-FeOOH) surface. Coll. Surf. 2, 101–117. doi:10.1016/0166-6622(81)80001-7

Smith, V H., 2009. Eutrophication. In: Gene E. Likens, (Editor) Encyclopedia of Inland Waters. Volume 3, pp. 61–73 Oxford: Elsevier.

Veli, S., Alyüz, B., 2007. Adsorption of copper and zinc from aqueous solutions by using natural clay. J. Hazard. Mater. 149(1), 226–233.

Weng, L., van Riemsdijk, W.H., Hiemstra, T., 2008. Humic nanoparticles at the oxide - water interface : interactions with phosphate ion adsorption. Environ. Sci. Technol. 42, 8747–8752.

Zamparas, M., Drosos, M., Georgiou, Y., Deligiannakis, Y., Zacharias, I., 2013. A novel bentonite-humic acid composite material Bephos® for removal of phosphate and ammonium from eutrophic waters. Chem. Eng. J. 225, 43–51. doi:10.1016/j.cej.2013.03.064

Figures

Fig. 1. Adsorption isotherms of the four adsorbents. Adsorbent concentration 1 g L^{-1}; pH =7. Standard deviation is represented by vertical bars.

Fig. 2. SEM image of Fe-Si-La particles.

Fig. 3. Magnetization curves of bare Fe_3O_4 and Fe-Si-La particles at 293K.

Fig. 4. P removal efficiency (Pr in %) for the merged data of all studied systems as a function of type of adsorbent and adsorbent dosage. Standard deviation is represented by vertical bars.

Fig. 5. Relation between adsorbed P and color for the four studied adsorbents. *r* is the Pearson correlation coefficient. The y-axis values are power-transformed (x^2).

Fig. 6. Relation between adsorbed P and NO_3^- for the four studied adsorbents. *r* is the Pearson correlation coefficient. The y-axis values are power-transformed (x^2).

Fig. 7. P removal efficiency (Pr in %) of non magnetic adsorbents (CFH-12® and Phoslock®) for each lake. High adsorbent dosage in black and low in grey. Standard deviation is represented by vertical bars.

Fig. 8. P removal efficiency (Pr in %) of magnetic adsorbents (Fe-Si-La and FeHQ) for each lake. High adsorbent dosage in black and low in grey. Standard deviation is represented by vertical bars.

Fig. 1

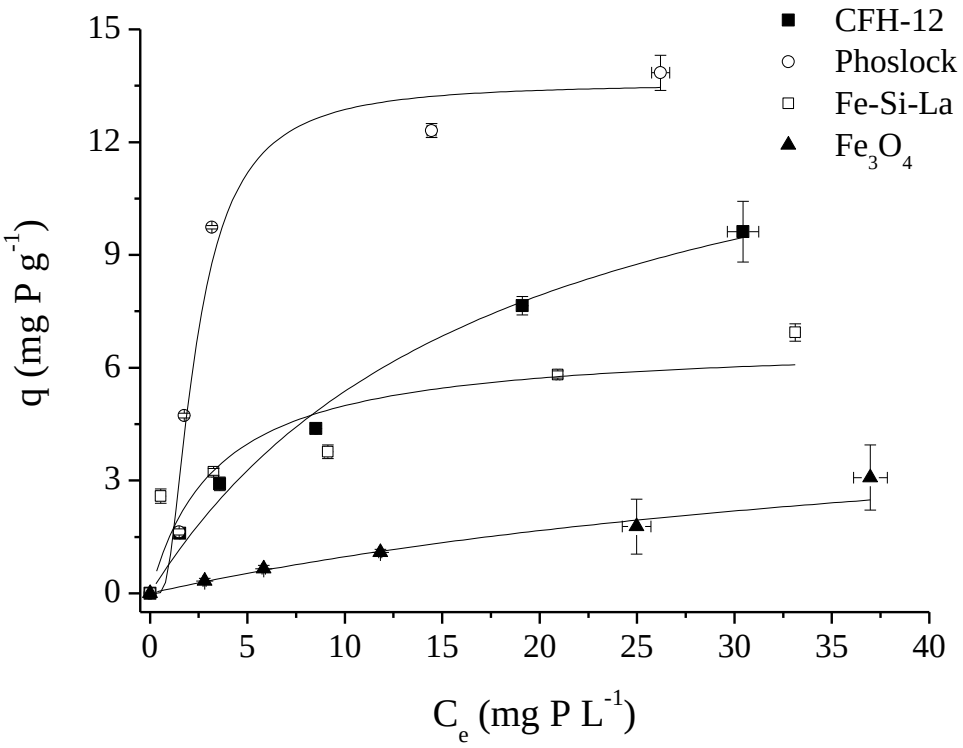
CFH-12
Phoslock
Fe-Si-La
Fe_3O_4
q (mg P g^{-1})
C_e (mg P L^{-1})
0
3
6
9
12
15
0
5
10
15
20
25
30
35
40

Fig.2

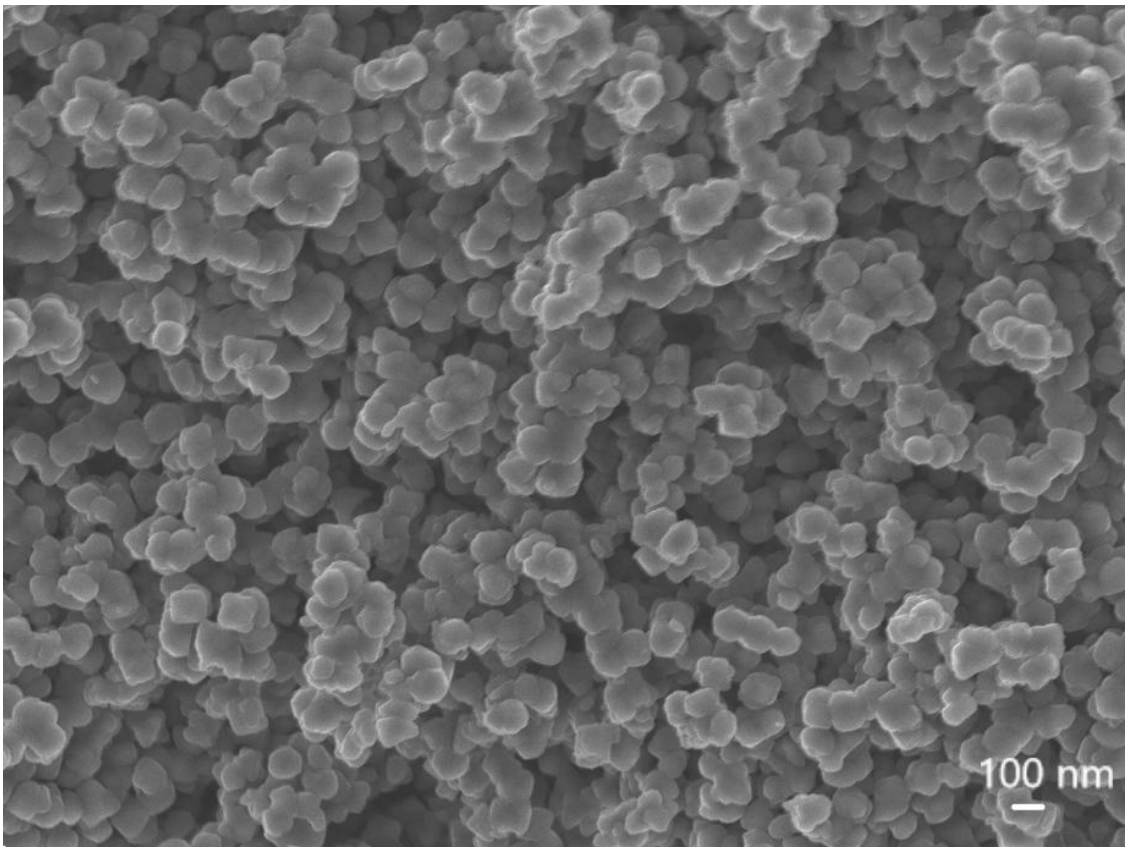

Fig.3

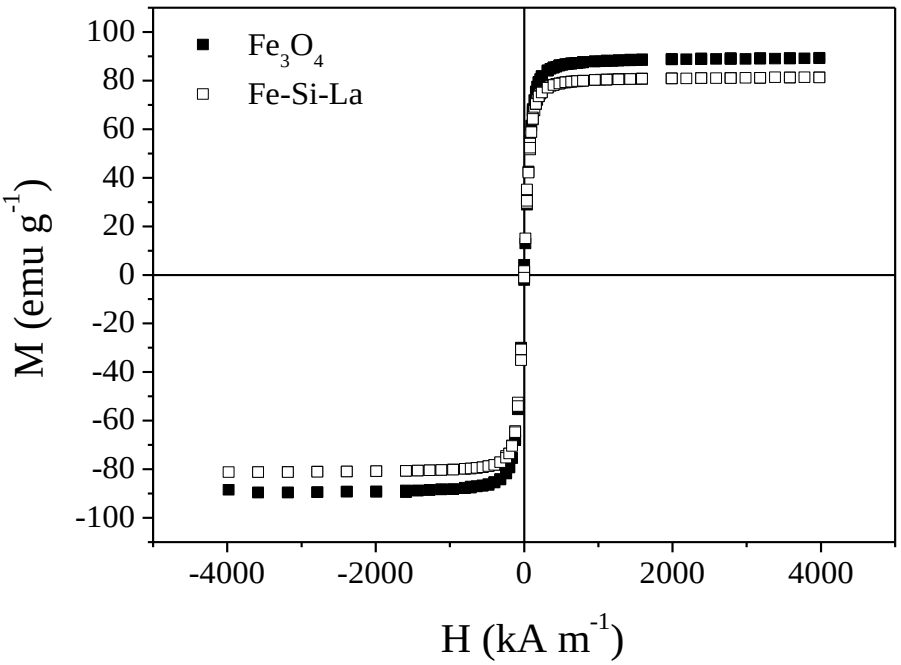
Fe3O4
Fe-Si-La
M (emu g-1)
H (kA m-1)
100
80
60
40
20
0
-20
-40
-60
-80
-100
-4000
-2000
0
2000
4000

Fig. 4

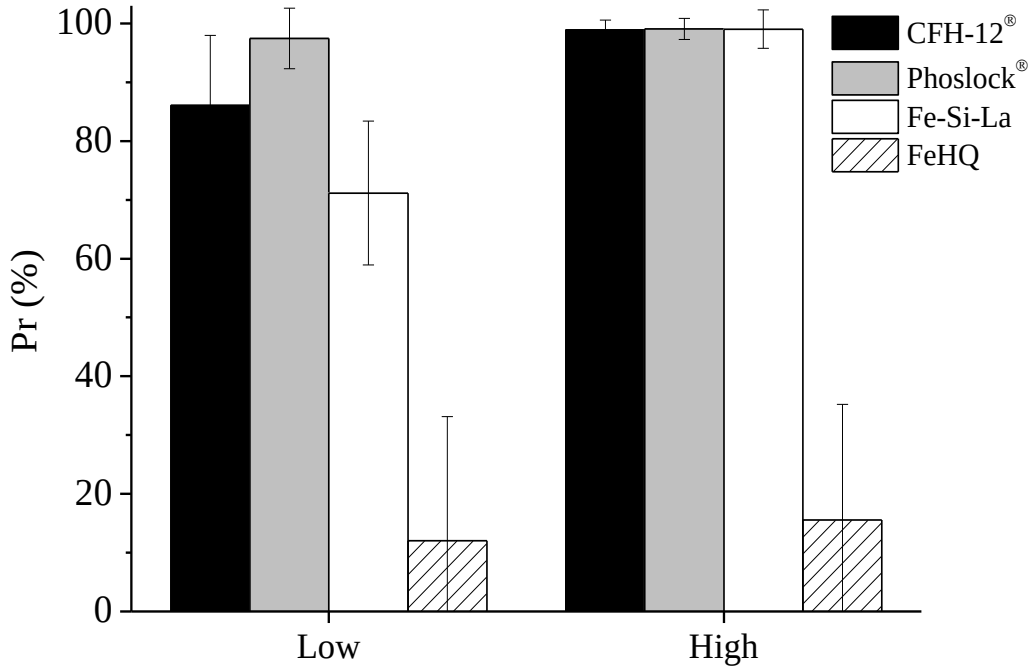

Fig. 5

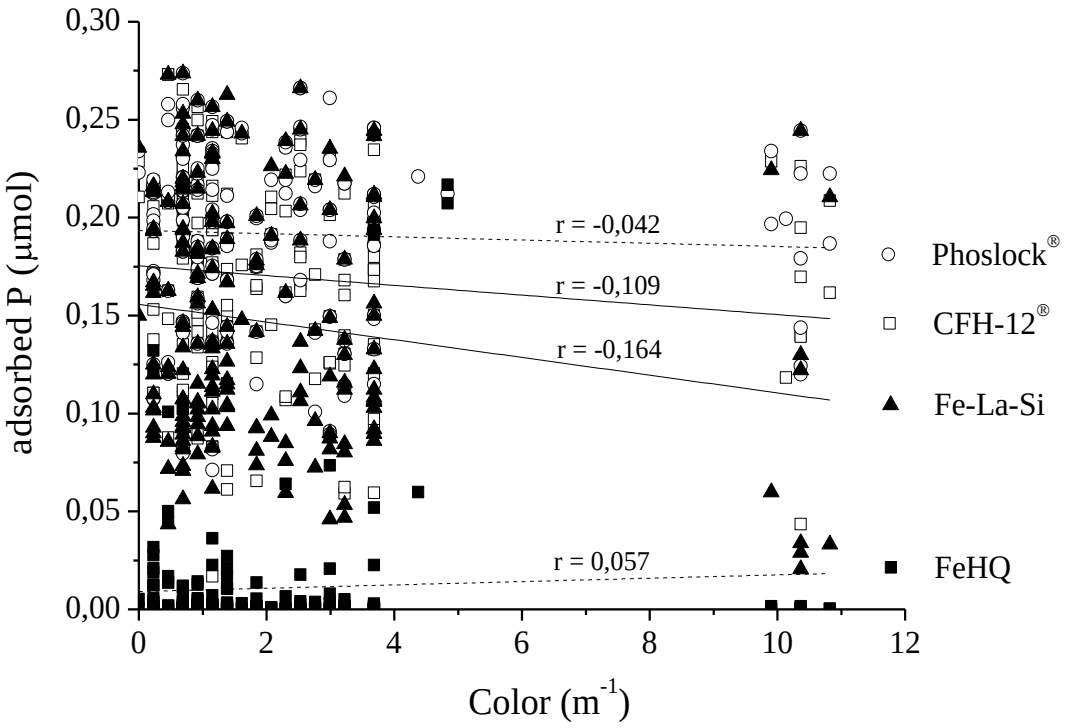
0,30
0,25
0,20
0,15
0,10
0,05
0,00
adsorbed P (µmol)
0
2
4
6
8
10
12
Color (m-1)
r = -0,042
r = -0,109
r = -0,164
r = 0,057
Phoslock®
CFH-12®
Fe-La-Si
FeHQ

Fig. 6

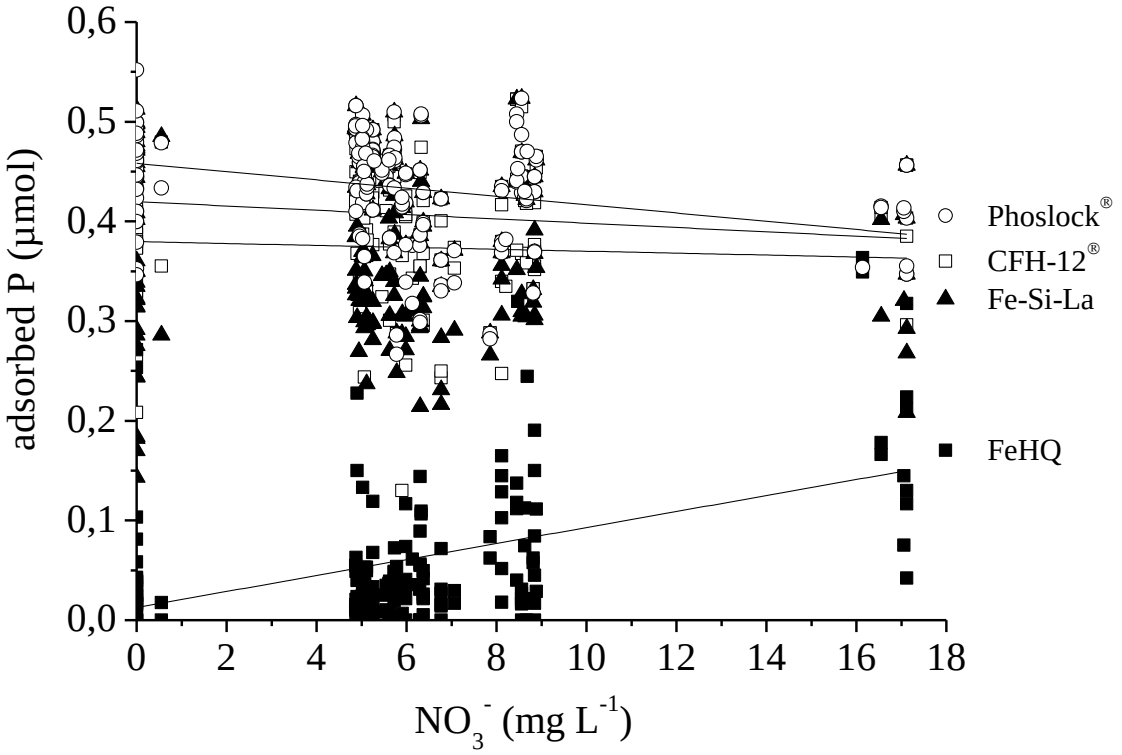
adsorbed P (µmol)
0,0
0,1
0,2
0,3
0,4
0,5
0,6
0
2
4
6
8
10
12
14
16
18
NO3- (mg L-1)
Phoslock®
CFH-12®
Fe-Si-La
FeHQ

Fig. 7

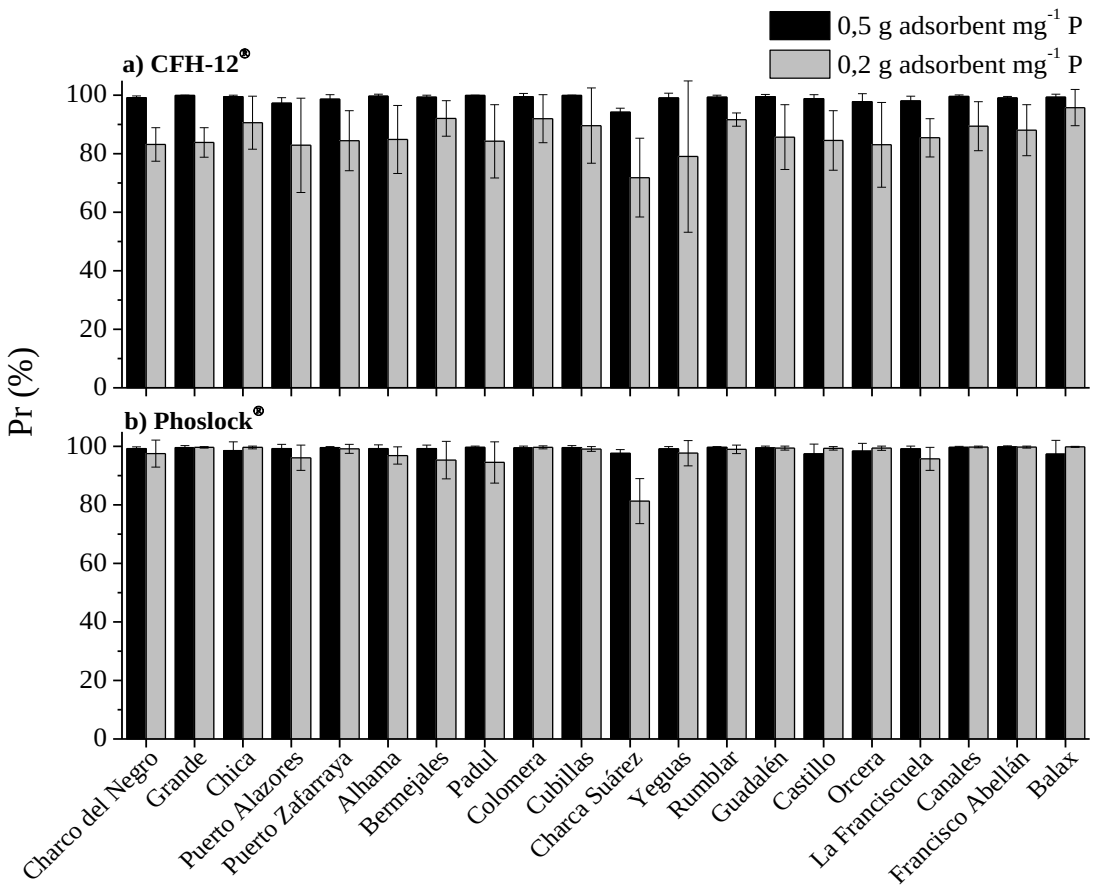
0,5 g adsorbent mg-1 P
0,2 g adsorbent mg-1 P
a) CFH-12®
b) Phoslock®
Pr (%)
0
20
40
60
80
100
Charco del Negro
Grande
Chica
Puerto Alazores
Puerto Zafarraya
Alhama
Bermejales
Padul
Colomera
Cubillas
Charca Suárez
Yeguas
Rumblar
Guadalén
Castillo
Orcera
La Francicuela
Canales
Francisco Abellán
Balax

Fig. 8

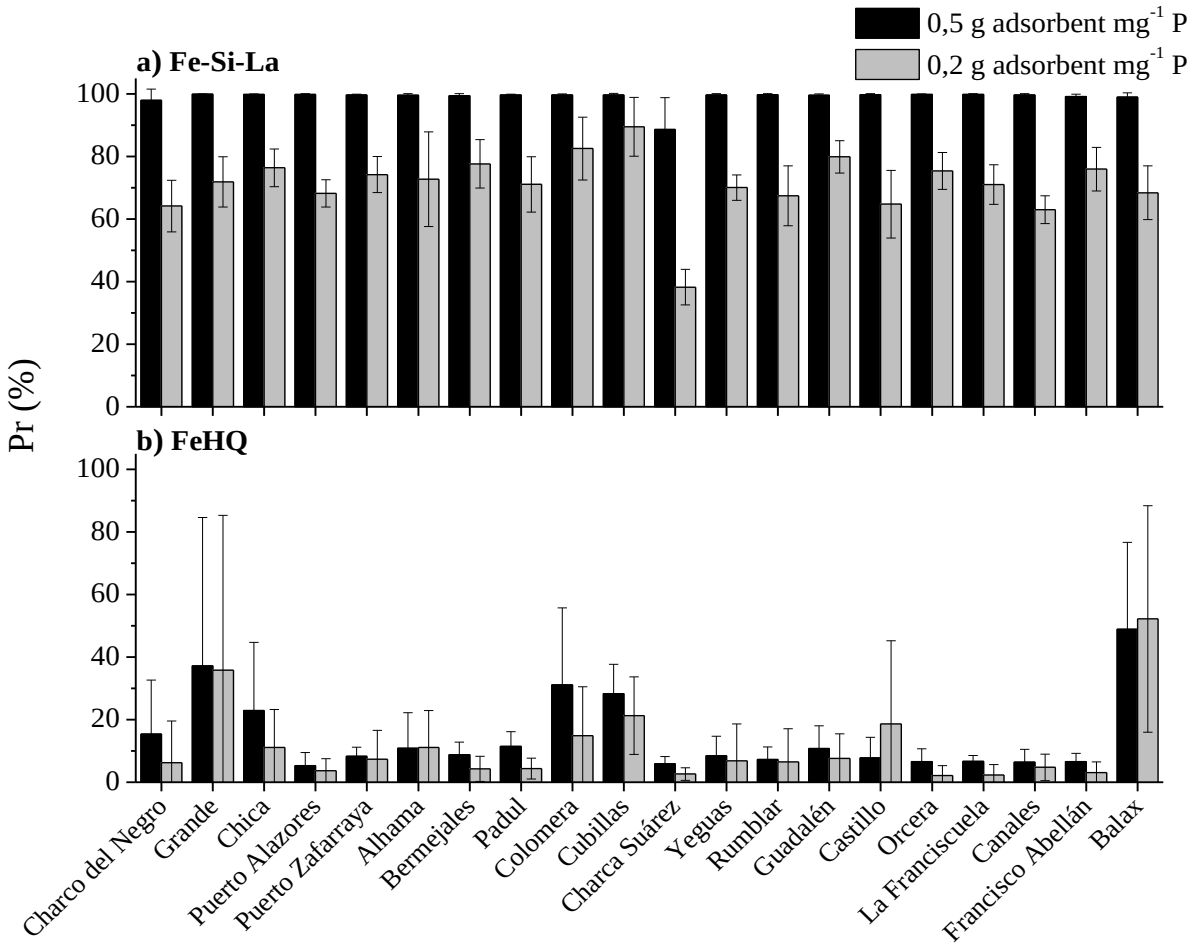
0,5 g adsorbent mg-1 P
0,2 g adsorbent mg-1 P
a) Fe-Si-La
b) FeHQ
Pr (%)
0
20
40
60
80
100
Charco del Negro
Grande
Chica
Puerto Alazores
Puerto Zafarraya
Alhama
Bermejales
Padul
Colomera
Cubillas
Charca Suárez
Yeguas
Rumblar
Guadalén
Castillo
Orcera
La Franciscuela
Canales
Francisco Abellán
Balax

Tables

Table 1. Chemical characterization of the studied lakes (average values of four analysis). The aquatic systems were classified according to Hammer et al. (1986) as freshwater (F), subsaline (S) or hyposaline (H) systems.

Table 2. Surface chemical composition (%) of bare Fe_3O_4 and Fe-Si-La particles by XPS.

Table 3. Best models predicting P adsorption obtained through model selection ($\Delta AIC_c < 2$). AIC_c values, AIC_c differences (Δ) and Akaike weights (ω) of the subset of models generated. *l* is the maximized log likelihood. (1) *type of adsorbent*, (2) *adsorbent dose*, (5) *color*, (7) NO_3^- *and* (11) $C_{cont.}$

Table 4. Model coefficients. Estimate (the model-based estimate for the coefficient for each parameter without weighting), standard error (SE), associated Wald's z score (z) and significance level (*p*) for the fixed factors explaining P adsorption.

Table 5. Post hoc analysis of the simple main effects for the interaction type adsorbent x adsorbent dosage. The Holm's method correction of *p* was used to protect the family-wise error rate.

Table 6. Post hoc analysis of the pairwise comparisons between the types of adsorbent for the interaction type adsorbent x NO_3^-. The Holm's method correction of *p* was used to protect the family-wise error rate.

Table 7. Relationships of each type of adsorbent with NO_3^- concentration for the interaction type adsorbent x NO_3^-.

Table 1

	Lake	pH	Conductivity $\mu S\ cm^{-1}$	PO_4^{3-} $\mu g\ L^{-1}$	Na^+ $mg\ L^{-1}$	K^+ $mg\ L^{-1}$	Mg^{2+} $mg\ L^{-1}$	Ca^{2+} $mg\ L^{-1}$	NO_3^- $mg\ L^{-1}$	Cl^- $mg\ L^{-1}$	SO_4^{2-} $mg\ L^{-1}$	Si $mg\ L^{-1}$	Color m^{-1}	Mn $\mu g\ L^{-1}$	As $\mu g\ L^{-1}$	Ni $\mu g\ L^{-1}$	Cu $\mu g\ L^{-1}$
1	**Charco del Negro (F)**	7.46	321	16.81	0.40	2.20	0.99	44.50	3.86	4.23	42.43	3.85	2.99	1.00	1.39	3.25	2.43
2	**Grande (H)**	6.97	3928	6.49	104.60	5.61	147.68	733.86	3.84	184.38	2268.67	9.32	2.82	74.87	3.23	29.40	6.96
3	**Chica (H)**	7.91	7415	0.00	543.03	12.22	352.44	727.31	7.36	991.16	2937.76	0.55	2.59	666.06	9.16	31.99	33.98
4	**Puerto Alazores (F)**	8.14	310	0.13	0.00	0.00	4.71	38.71	2.44	6.85	19.54	2.28	1.61	0.79	1.32	2.86	1.77
5	**Puerto Zafarraya (F)**	8.10	332	3.95	5.80	0.86	3.79	39.70	1.82	12.43	11.71	0.00	1.23	0.99	0.98	3.08	1.21
6	**Alhama (F)**	8.26	359	0.00	0.00	0.00	12.71	42.94	8.49	5.31	14.66	2.53	0.46	0.79	1.18	2.08	0.35
7	**Bermejales (S)**	8.26	549	0.00	0.00	0.61	29.65	57.43	5.74	7.06	135.75	1.08	0.38	0.71	1.57	3.63	0.65
8	**Padul (S)**	8.30	574	4.08	0.93	0.91	33.38	58.00	6.65	10.22	38.85	0.73	3.07	1.10	3.06	4.37	0.95
9	**Colomera (S)**	8.05	656	0.00	15.69	1.75	17.92	66.84	8.76	35.02	157.54	1.46	0.58	0.78	1.48	4.68	1.81
10	**Cubillas (S)**	8.11	686	0.00	7.48	1.19	25.48	78.34	8.21	20.74	161.07	1.70	0.92	0.52	1.61	5.79	1.07
11	**Charca Suárez (S)**	8.01	1474	141.54	95.86	19.10	57.07	81.89	0.00	192.32	130.41	10.10	10.31	3.22	11.07	6.18	6.57
12	**Yeguas (F)**	7.57	110	0.13	0.09	0.00	0.29	3.96	5.92	7.16	11.73	2.44	1.21	0.90	3.65	0.91	1.29
13	**Rumblar (F)**	7.30	235	0.00	0.24	0.25	6.41	15.45	5.25	8.04	59.64	0.00	0.77	0.85	2.66	2.39	1.77
14	**Guadalén (F)**	7.84	353	1.40	8.69	2.85	11.44	28.67	6.33	17.12	45.34	0.00	0.77	0.69	1.82	4.20	1.69
15	**Castillo (S)**	7.24	798	1.53	3.47	14.20	25.48	95.12	1.22	16.01	336.97	0.02	2.25	2.79	3.29	7.92	13.85
16	**Orcera (S)**	8.08	678	0.00	0.00	6.74	31.93	75.78	5.06	15.00	164.16	0.34	3.28	1.68	3.27	5.97	1.43
17	**La Franciscuela (F)**	8.13	336	0.00	0.00	0.00	9.40	41.87	3.35	4.27	12.39	0.38	1.00	0.57	0.41	2.62	0.14
18	**Canales (F)**	7.77	179	9.04	0.00	0.00	1.99	16.97	5.11	4.43	25.32	0.21	0.38	1.47	1.20	1.28	0.15
19	**Francisco Abellán (S)**	8.20	565	0.00	1.86	0.62	29.06	54.84	5.59	12.33	114.42	0.15	0.46	0.46	1.26	3.25	0.38
20	**Balax (F)**	5.82	101	5.22	0.00	0.10	0.33	5.41	16.72	5.16	22.35	3.03	0.29	52.52	0.77	6.92	0.46

Table 2

	Fe	O	C	Si	La
Fe_3O_4	9.63	31.41	58.96	-	-
Fe-Si-La	3.54	49.52	28.59	13.00	5.34

Table 3

Model	l	$\mathbf{AIC}_c$	$\Delta\mathbf{AIC}_c$	ω
(A)1*+2*+1 x 2*+11*	1666.84	-30308.98	0.00	0.49
(B)1*+2*+1 x 2*+11*+7+1 x 7*	1669.92	-30307.17	1.82	0.20
(C)1*+2*+1 x 2*+11*+5*	1666.74	-303.04	1.95	0.19

* $p<0.001$

Table 4

Fixed Factors	df	χ^2	*p*
Intercept			
Type of adsorbent	3	2663.60	< 0.001
Adsorbent dosage	1	156.66	< 0.001
C_{cont}	1	794.28	< 0.001
Color	1	39.36	< 0.001
NO_3^-	1	0.21	0.6
Type of adsorbent x NO_3^-	3	50.26	< 0.001
Type of adsorbent x adsorbent dosage	3	509.95	< 0.001

Table 5

	Value	df	χ^2	*p*
CFH-12®	0.0416	1	156.66	< 0.001
Phoslock®	0.0063	1	3.80	0.102
Fe-Si-La	0.0949	1	807.43	< 0.001
FeHQ	0.0008	1	0.05	0.819

Table 6

	Value	df	χ^2	*p*
CFH-12® - Fe-Si-La	-0.0006	1	0.78	0.376
CFH-12® - FeHQ	-0.0030	1	21.33	< 0.001
CFH-12® - Phoslock®	0.0014	1	5.22	< 0.050
Phoslock® - FeHQ	0.0044	1	48.79	< 0.001
Phoslock® - Fe-Si-La	0.0020	1	10.14	< 0.010
Fe-Si-La - FeHQ	0.0024	1	13.92	< 0.001

Table 7

	Value	df	χ^2	*p*
CFH-12®	-0.0002	1	0.21	0.936
Phoslock®	-0.0017	1	12.83	< 0.010
Fe-Si-La	0.0003	1	0.53	0.936
FeHQ	0.0028	1	32.41	< 0.001